Research Square

Preprints are preliminary reports that have not undergone peer review.
They should not be considered conclusive, used to inform clinical practice,
or referenced by the media as validated information.

A Five-Point Method for Estimating DC, Fundamental, and Third-Harmonic Parameters of Electromagnetic-Field Signals at a Known Frequency

Weihao Zhang

zhangweihaofzu@126.com

State Grid Fujian Electric Power Research Institute

Wenbin Wu

State Grid Fujian Electric Power Research Institute

Xiaojie Wu

State Grid Fujian Electric Power Company

Renshu Wang

State Grid Fujian Electric Power Research Institute

Article

Keywords: five-point method, known-frequency parameter estimation, DC component, fundamental component, third harmonic, electromagnetic-field measurement

Posted Date: November 19th, 2026

DOI: https://doi.org/10.21203/rs.3.rs-11585940/v1

License: This work is licensed under a Creative Commons Attribution 4.0 International License.
Read Full License

Additional Declarations: No competing interests reported.

A Five-Point Method for Estimating DC, Fundamental, and Third-Harmonic Parameters of Electromagnetic-Field Signals at a Known Frequency

Weihao Zhang[1,*], Wenbin Wu[1], Xiaojie Wu[2], and Renshu Wang[1]

[1]State Grid Fujian Electric Power Research Institute, No. 48 Fuyuan Branch Road, Cangshan District, Fuzhou 350007, China

[2]State Grid Fujian Electric Power Company, No. 257 Wusi Road, Gulou District, Fuzhou 350003, China

[*]Corresponding author: Weihao Zhang (e-mail: zhangweihaofzu@126.com)

Keywords: five-point method; known-frequency parameter estimation; DC component; fundamental component; third harmonic; electromagnetic-field measurement

I Abstract

To estimate electromagnetic-field signal parameters within a short observation window, this paper presents a five-point method for signals with a known fundamental frequency. The signal model, comprising a DC component, a fundamental component, and a third harmonic, is expressed as a linear combination of sine and cosine basis functions. Five equally spaced samples form a 5 × 5 linear system, which is solved to obtain the DC component and the amplitudes and initial phases of the fundamental and third-harmonic components. The solution matrix can be calculated in advance from the sampling interval and known frequency to reduce real-time computation; the sampling interval must be selected so that the coefficient matrix is nonsingular and suitably conditioned. MATLAB/Simulink simulations were used to examine fundamental-only, third-harmonic, and time-varying-amplitude signals, while a parallel-plate power-frequency electric-field platform was used to evaluate steady-state and dynamic measurements. The results show that, when the signal follows the assumed model and the fundamental frequency is known, the method estimates the parameters from five samples. At a sampling interval of 1 ms, the first-to-last sample span is 4 ms, allowing changes in the electric-field amplitude to be observed. The method does not estimate frequency, and its practical accuracy depends on noise, sampling interval, matrix conditioning, and sensor errors.

II Introduction

Unmanned aerial vehicle (UAV) inspection is increasingly used to monitor and maintain overhead transmission lines. Electric- or magnetic-field information can support line detection, localization, and UAV control, complementing conventional vision-based inspection[1-4]. The electromagnetic environment near transmission lines may also affect UAVs and their sensors, making it important to characterize the fields and assess measurement performance[5,6]. Previous studies have used electric-field sensor arrays, integrated electric-field sensors, and tunneling magnetoresistive sensors to obtain line-related information, applying electromagnetic-field measurements to UAV localization and transmission-line parameter reconstruction[1-6]. These studies show that field measurement accuracy can affect both field-strength estimation and UAV positioning and operation near lines.

Periodic signals containing harmonics are commonly analyzed using spectral methods, sinusoidal fitting, or parameter-estimation techniques. Li et al. studied computationally efficient parameter estimation for harmonic sinusoidal signals[7]. Ramos et al. proposed multiharmonic least-squares fitting and evaluated its performance through simulations and experiments[8], with later work improving its convergence[9]. For short sinusoidal records, Chen et al. investigated initializing sine-wave fitting with frequency information obtained from an FFT[10]. In power-system applications, Kalman filtering and other parameter-estimation methods have been used to track harmonic variations and estimate harmonic levels in distribution systems[11-13]. These methods extend the range of harmonic-estimation applications, but differ in their sampling requirements, computational procedures, and estimated parameters.

When the signal frequency is known, linear least-squares methods can reduce the complexity of sinusoidal parameter estimation. Belega et al. studied frequency-domain linear least-squares estimation of the amplitude and phase of real-valued sinusoids [14] and analyzed accuracy bounds under known- and unknown-frequency, coherent- and noncoherent-sampling conditions[15]. Fast estimation methods have also been developed for signals affected by noise or harmonic distortion, including studies of short records, noise, and harmonic interference[16-18]. Recent work has further examined short-record sinusoidal estimation, harmonic phasor estimation, and measurement uncertainty, including damped-sinusoid estimation, single-cycle phasor estimation, harmonic and interharmonic estimation, and uncertainty in known-frequency amplitude and phase estimates[19-22]. These studies indicate that reducing observation time requires consideration of estimation error, noise, and sampling conditions.

Most existing studies address single-frequency sinusoidal estimation, general multiharmonic fitting, harmonic-phasor tracking, or harmonic-state estimation at the power-system level. For short measurement records that must be processed rapidly during UAV inspection, a dedicated analysis of the sampling structure and parameter identifiability is still needed when the fundamental frequency is known and only five samples are used to jointly estimate the DC, fundamental, and third-harmonic parameters. This paper therefore formulates a known-frequency five-point signal model, derives the corresponding parameter-solving method, and evaluates its estimation performance through simulations and experiments. The aim is to provide a short-record parameter-estimation approach for rapid electromagnetic-field signal processing in UAV-based transmission-line inspection.

III Existing Methods for Electromagnetic-Field Signal Parameter Estimation

Existing approaches for extracting parameters from composite sinusoidal electromagnetic-field signals mainly include time-domain fitting, spectral analysis, and filtering. This section outlines their principles and conditions of use to provide a basis for the known-frequency five-point method developed below.

A Time-Domain Fitting Methods

Time-domain fitting uses a sum-of-sinusoids model and fits it to sampled data to estimate the DC component and the amplitudes, frequencies, and phases of individual harmonics. A composite electromagnetic-field signal measured by a UAV can be written as follows:

$$y(t)=A_0+\sum_{k=1}^{m} A_k \sin\left(k\omega_0 t+\varphi_k\right) \tag{1}$$

where A_0 is the DC component; A_k is the amplitude of the k-th harmonic; ω_0 is the fundamental angular frequency; φ_k is the phase of the k-th harmonic; and m is the highest harmonic order, set to 3 in this study.

Least-squares and nonlinear least-squares methods are commonly used for fitting, with least squares being particularly widespread. The method constructs a residual objective function and minimizes it:

$$J=\sum_{i=1}^{N}\left[y_i-\hat{y}_i\right]^2 \tag{2}$$

where y_i is the measured value of the ith sample, $\hat{y}_i$ is the corresponding model estimate, and N is the number of samples. Minimizing the objective yields estimates of the unknown parameters.

For the discrete composite signal model with unknown phases, nonlinear least squares is generally used. The sum of squared residuals is defined as:

$$J(p)=\sum_{i=1}^{N}\left[y(t_i)-\left(A_0+\sum_{k=1}^{m} A_k \sin\left(k\omega_0 t_i+\varphi_k\right)\right)\right]^2 \tag{3}$$

The objective-function derivatives with respect to the estimated parameters can be evaluated using gradient descent, with the parameters iteratively updated in the negative-gradient direction until the objective converges to a local minimum. The resulting estimates include the DC component, harmonic amplitudes, fundamental angular frequency, and phases. Although this method can provide accurate parameter fitting under steady-state conditions, its computational complexity increases substantially with harmonic order. It is also sensitive to

initial parameter values and convergence conditions, which can make iterative computation unsuitable for rapid processing during UAV inspection.

B Spectral Analysis Methods

Spectral analysis is a classical approach to harmonic extraction. It maps a time-domain waveform to the frequency domain using the Fourier transform and related algorithms, allowing DC, fundamental, and harmonic components to be separated and estimated. The continuous Fourier transform is expressed as:

$$F(\omega)=\int_{-\infty}^{+\infty} y(t)\, e^{-j\omega t}dt \tag{4}$$

where $y(t)$ is the time-domain signal, ω is angular frequency, and $F(\omega)$ is the corresponding frequency-domain signal. For a discrete sequence, the discrete Fourier transform (DFT) is used:

$$X(k)=\sum_{n=0}^{N-1} x(n)e^{-j\frac{2\pi}{N}kn} \tag{5}$$

where N is the number of samples, $x(n)$ is the nth sample, and $X(k)$ is the result at frequency bin k.

The fast Fourier transform (FFT) is an efficient implementation of the DFT that reduces computational cost through butterfly operations. Applying the FFT to sampled data yields a spectrum from which the fundamental and harmonic parameters can be extracted. Window functions such as the Hann and Hamming windows can reduce spectral leakage, although their effects on amplitude estimates must be corrected.

FFT methods and their variants require a fixed-length observation window, usually spanning one or more signal periods. When a UAV moves rapidly and the field amplitude changes, a long window can delay amplitude and phase updates and obscure the instantaneous field characteristics. FFT alone may therefore be insufficient for real-time measurement under highly dynamic conditions.

C Filtering Methods

Filtering methods use the frequency-selective characteristics of digital filters to separate the DC component, fundamental, and target harmonics. The amplitude and phase of each filtered component are then analyzed in the time domain. A general digital difference equation is given by:

$$\sum_{i=0}^{M} a_i y(n-i)=\sum_{j=0}^{N} b_j x(n-j) \tag{6}$$

where $x(n)$ is the input signal, $y(n)$ is the filter output, a_i and b_j are filter coefficients, and M and N are the denominator and numerator orders, respectively. For an FIR filter, $a_0=1$ and $a_i=0$ for $i > 0$.

In practice, a low-pass filter with a cutoff below the power frequency can extract the DC component, while band-pass filters centered at the fundamental and third-harmonic frequencies can isolate the target components. The filter outputs can then be used to estimate amplitude and phase.

Digital filters used in engineering include finite impulse response (FIR) and infinite impulse response (IIR) filters. FIR filters have no feedback path and are unconditionally stable, but achieving sharp transition bands and strong stopband attenuation often requires a high filter order, increasing computation and processor-resource requirements.

IIR filters use recursive feedback and generally require a lower order than FIR filters for comparable specifications, reducing computation and resource use in embedded real-time processing. However, IIR filters have a transient settling period. In dynamic UAV field measurements, this settling behavior can limit tracking of rapid field changes and introduce measurement error.

In summary, existing methods involve trade-offs among observation duration, computational cost, and dynamic response. This study examines how to estimate parameters rapidly from a limited number of equally spaced samples when the fundamental frequency is known, and the signal model includes a DC component and specified harmonics.

IV Signal Model and Algorithm

A Mathematical Model of the Electromagnetic-Field Signal

The electromagnetic-field measurement signal near a transmission line can be modeled as the superposition of several components in the same measurement channel. To describe the sensor zero offset and the principal periodic components, this study uses a finite-dimensional model comprising a DC component, the power-frequency fundamental, and the third harmonic. The objective is to estimate the amplitudes and initial phases of these components from a short set of discrete samples, assuming that the fundamental frequency is known. Thus, frequency is an input to the model rather than a parameter estimated by the proposed method.

The third harmonic is included to represent a possible source of waveform distortion. Its significance depends on the spectral characteristics of the measurement target; the model does not assume that the third harmonic dominates in every transmission-line environment. If other harmonics or interharmonics are significant in a particular application, they should be added to the model, with a corresponding increase in the number of unknown parameters and sample equations.

Considering these components, the measured time-domain signal at an arbitrary time t is expressed as follows:

$$y(t)=A_0+A_1\sin(\omega t+\varphi_1)+A_3\sin(3\omega t+\varphi_3) \tag{7}$$

where $y(t)$ is the instantaneous measured signal; A_0 is the DC offset; A_1 and φ_1 are the amplitude and initial phase of the fundamental, respectively; and A_3 and φ_3 are the amplitude and initial phase of the third harmonic, respectively. The fundamental angular frequency is $\omega=2\pi f$, where f is known, and the third-harmonic angular frequency is 3ω. For a 50 Hz signal, $\omega=100\pi rad/s$. The parameters are assumed to remain approximately constant within each five-sample window; this local-stationarity assumption underlies the short-window solution.

In the original signal model, the amplitudes and phases appear as coupled terms within the sinusoidal functions. If φ_1 and φ_3 are directly treated as unknown parameters, the resulting measurement equations are nonlinear with respect to these phases and cannot be solved using a single linear matrix operation. To transform the problem into a linear parameter estimation problem, the trigonometric addition identities are applied to the fundamental and third-harmonic components, yielding

$$\sin(\omega t+\varphi_1)=\sin(\omega t)\cos\varphi_1+\cos(\omega t)\sin\varphi_1,\ \sin(3\omega t+\varphi_3)=\sin(3\omega t)\cos\varphi_3+\cos(3\omega t)\sin\varphi_3. \tag{8}$$

Since the angular frequency ω is known, the sine and cosine terms at each sampling instant can be directly calculated. Consequently, the unknown parameters are confined to the coefficients associated with the amplitudes and phases.

Substituting the expanded expressions into the original signal model allows each frequency component to be represented as a linear combination of sine and cosine basis functions. Accordingly, the following equivalent coefficients are introduced:

$$\begin{cases} B_1=A_1\cos\varphi_1, C_1=A_1\sin\varphi_1, \\ B_3=A_3\cos\varphi_3, C_3=A_3\sin\varphi_3. \end{cases} \tag{9}$$

Using these coefficients, the signal model can be rewritten as

$$y(t)=A_0+B_1\sin(\omega t)+C_1\cos(\omega t)+B_3\sin(3\omega t)+C_3\cos(3\omega t). \tag{10}$$

The resulting model is linear with respect to the five unknown coefficients A_0, B_1, C_1, B_3, and C_3. Since the fundamental angular frequency is known, all five basis functions can be evaluated at any given sampling instant. Therefore, five measurements acquired at distinct sampling instants can be used to construct a system of five linear equations for estimating these coefficients, provided that the corresponding coefficient matrix has full rank. The transformed model is linear in its unknown coefficients. Define the parameter vector $X=[A_0, B_1, C_1, B_3, C_3]^T$, where A_0 represents the DC offset, B_1 and C_1 are the fundamental sine and cosine coefficients, and B_3 and C_3 are the corresponding third-harmonic coefficients. The amplitudes and phases have thus been recast as five linear coefficients, from which the physical parameters can be recovered by an inverse transformation.

Five unknown parameters require at least five independent observations. Independence here requires the coefficient matrix formed from the basis functions to have full rank; distinct sampling times alone do not

guarantee this. In particular, $det(M)$ must be nonzero. If the sampling interval causes basis-function columns to become dependent or nearly dependent, the matrix is singular or ill-conditioned, and the parameters cannot be determined uniquely or robustly. With five samples and five unknowns, the system is exactly determined: it has an exact solution when the model holds and the data are noise-free. Measurement noise, quantization, or unmodeled components perturb the solution, and the condition number of M affects the resulting error amplification.

B Construction and Solution of the Linear System

The signal is sampled at a fixed interval Δt. Let $y(t_1), \ldots, y(t_5)$ be five consecutive, equally spaced samples, where $t_{i+1}=t_i+\Delta t$. Substituting each sampling time into the linearized model gives one linear equation in A_0, B_1, C_1, B_3, and C_3. The five equations together form the system to be solved.

Arranging the five scalar equations by sampling time and placing the values of each basis function in the corresponding matrix column gives the standard matrix form:

$$Y=MX \tag{11}$$

Here, $Y=[y(t_1), y(t_2), y(t_3), y(t_4), y(t_5)]^{\mathrm{T}}$ is the observation vector; $X=[A_0, B_1, C_1, B_3, C_3]^{\mathrm{T}}$ is the unknown-parameter vector; and M is a 5×5 coefficient matrix. M is determined by the known angular frequency ω and the sampling times, and is independent of the measured amplitudes. Its columns correspond, in order, to the constant, fundamental sine, fundamental cosine, third-harmonic sine, and third-harmonic cosine basis functions.

The *i-th* row of M contains the values of the five basis functions at time t_i: the constant function 1, $\sin \omega t_i$, $\cos \omega t_i$, $\sin 3\omega t_i$, and $\cos 3\omega t_i$. Multiplying this row by X gives the linearized signal equation for the sample $y(t_i)$.

$$M_i=[1 \quad \sin \omega t_i \quad \cos \omega t_i \quad \sin 3\omega t_i \quad \cos 3\omega t_i] \tag{12}$$

Using the row definition above, the five sampling times form the following complete coefficient matrix:

$$M=\begin{bmatrix} 1 & \sin \omega t_1 & \cos \omega t_1 & \sin 3\omega t_1 & \cos 3\omega t_1 \\ 1 & \sin \omega t_2 & \cos \omega t_2 & \sin 3\omega t_2 & \cos 3\omega t_2 \\ 1 & \sin \omega t_3 & \cos \omega t_3 & \sin 3\omega t_3 & \cos 3\omega t_3 \\ 1 & \sin \omega t_4 & \cos \omega t_4 & \sin 3\omega t_4 & \cos 3\omega t_4 \\ 1 & \sin \omega t_5 & \cos \omega t_5 & \sin 3\omega t_5 & \cos 3\omega t_5 \end{bmatrix} \tag{13}$$

Equivalently, the *i-th* scalar equation is $y(t_i)=A_0+B_1 \sin \omega t_i+C_1 \cos \omega t_i+B_3 \sin 3\omega t_i+C_3 \cos 3\omega t_i$. Taking $i=1,\ldots,5$ gives the five rows of M. The sampling times must place the basis functions at distinguishable phase positions; simply choosing five different timestamps does not guarantee full rank.

When M has full rank, the system has a unique solution. The solution can be written as follows. In numerical implementations, however, solving $MX=Y$ with a linear solver, such as LU or QR factorization, is preferable to explicitly computing M^{-1} because it avoids unnecessary numerical error:

$$X=M^{-1}Y \tag{14}$$

With measurement error, an exactly determined five-point solution maps the noise in all five samples directly into the estimated parameters and has no redundant samples to average. The condition number can be used to assess sensitivity to error, and Δt should be selected to avoid a nearly singular matrix. The estimation error should be evaluated under the intended frequency, sampling interval, and noise conditions.

The solution gives the linearized coefficients A_0, B_1, C_1, B_3, and C_3. From $B=A\cos\varphi$ and $C=A\sin\varphi$, the amplitudes are recovered as the vector magnitudes, and the initial phases are recovered using atan2(C, B), which preserves the correct quadrant:

$$\begin{cases} A_1=\sqrt{B_1^2+C_1^2}, \varphi_1=\arctan 2\,(C_1,B_1) \\ A_3=\sqrt{B_3^2+C_3^2}, \varphi_3=\arctan 2\,(C_3,B_3) \end{cases} \tag{15}$$

The function arctan 2 (y,x) accounts for the quadrant and avoids the ambiguity of arctan(C/B), especially when B is near zero. If phase is reported in [0, 2π), add 2π to negative values. When a harmonic amplitude is zero, its phase is physically undefined and should not be interpreted independently.

C Fast Implementation with a Fixed Sampling Sequence

If arbitrary absolute sampling times are used, the trigonometric basis values and coefficient matrix must be recalculated for each acquisition. To reduce this repeated computation, the first sample in each window is assigned a local time of zero and the sampling interval is kept fixed. The coefficient matrix then depends only on the known frequency and Δt, so it can be computed in advance and reused for every window.

Using local time $\tau=t-t_1$, the five sampling times are $\tau_i=(i-1)\Delta t, i=1,\ldots,5$. This time shift does not change the estimated amplitudes, but the recovered phases are referenced to the start of the window. To express them relative to the global time origin, use $\varphi_{1,\text{global}}=\varphi_{1,\text{local}}-\omega t_1$; for the third harmonic, use $\varphi_{3,\text{global}}=\varphi_{3,\text{local}}-3\omega t_1$.

Substituting the standardized sampling times into the basis functions gives a fixed-form coefficient matrix determined only by ω and Δt:

$$M=\begin{bmatrix} 1 & 0 & 1 & 0 & 1 \\ 1 & \sin\omega\Delta t & \cos\omega\Delta t & \sin 3\omega\Delta t & \cos 3\omega\Delta t \\ 1 & \sin 2\omega\Delta t & \cos 2\omega\Delta t & \sin 6\omega\Delta t & \cos 6\omega\Delta t \\ 1 & \sin 3\omega\Delta t & \cos 3\omega\Delta t & \sin 9\omega\Delta t & \cos 9\omega\Delta t \\ 1 & \sin 4\omega\Delta t & \cos 4\omega\Delta t & \sin 12\omega\Delta t & \cos 12\omega\Delta t \end{bmatrix} \tag{16}$$

When ω and Δt are fixed and the matrix is adequately conditioned, the solution operator can be computed offline and stored. During online processing, each new five-sample window is arranged as Y and used to solve for X; the amplitudes and phases are then recovered from the B and C coefficients. For continuous processing, the window advances by one sample whenever a new measurement arrives. With Δt= 1 ms, the first-to-last sample span is 4 ms; an estimate is available after the fifth sample and can then be updated at each subsequent sampling instant. This short span avoids waiting for a complete 20 ms power-frequency cycle.

VSimulation and Experimental Results

A Simulation Results

A MATLAB/Simulink model was developed to evaluate the correctness, parameter-estimation performance, and practical implementation of the proposed method under steady-state and dynamic conditions. The target signal in the high-voltage transmission environment is primarily the power-frequency electromagnetic field radiated by the line. High-frequency interference from the environment and UAV motors can be filtered at the sensor input; therefore, it was not included in the simulation model. A signal generator produced standard sinusoidal signals to represent measurements from an onboard electromagnetic-field sensor, and a Function block implemented the proposed algorithm. The simulation model is shown in Figure 1.

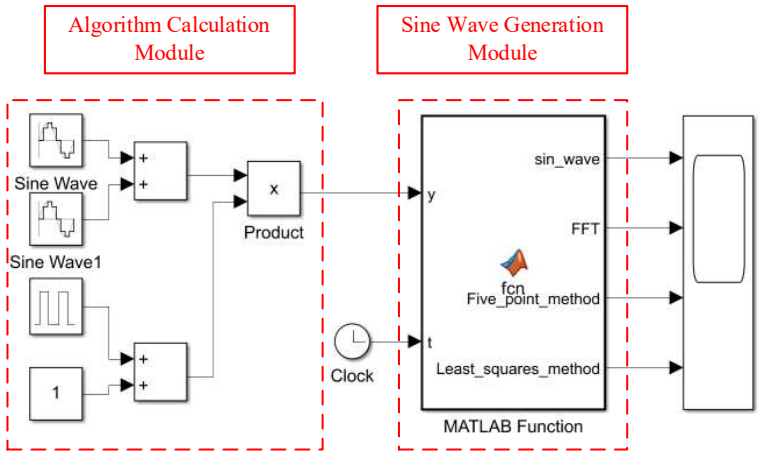


Figure 1. Simulation model of the five-point parameter-estimation method

The simulated power-frequency signal had a frequency of 50 Hz and an amplitude of 5 V, and the sampling interval for the five-point method was 1 ms. The proposed method was compared with a conventional FFT and a

known-frequency least-squares method. The FFT used a 20 ms, single-cycle observation window, while the least-squares method used a 3 ms window. The parameter-estimation results are shown in Figure 2.

Figure 2 shows that, for a single sinusoid with a known fundamental frequency of 50 Hz, the five-point method estimates the signal parameters from five equally spaced samples. Because this test signal contains no third harmonic, the theoretical third-harmonic amplitude is zero. Figure 3 shows the parameter estimates for a signal containing a third harmonic. In this case, the method jointly solves the sine and cosine coefficients of the fundamental and third harmonic. When the input frequency is known and the coefficient matrix is nonsingular, the amplitudes and initial phases of both components can be recovered.

Figure 4 shows simulation results for a signal with a third harmonic and a varying amplitude. The estimated amplitude changes as the signal amplitude changes, illustrating the parameter-estimation trend under amplitude variation. The five samples span $4\Delta t$; if the amplitude changes substantially within this interval, the assumption that the parameters remain approximately constant over the observation window may no longer hold, which can affect the estimates. Dynamic tracking performance should therefore be evaluated in relation to the sampling interval, amplitude-change rate, and estimation error.

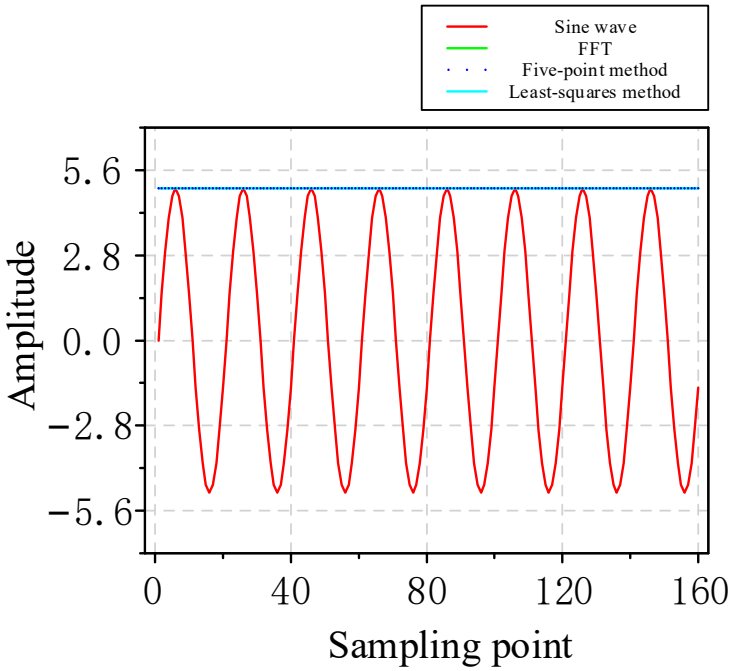


Figure 2. Sampled sinusoidal signal and estimated amplitude

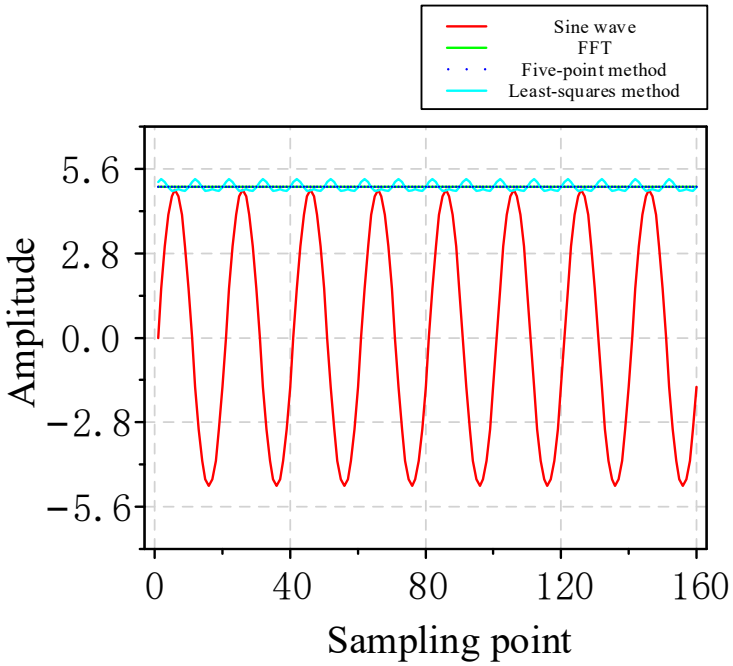


Figure 3. Sampled signal and estimated amplitude with a third harmonic

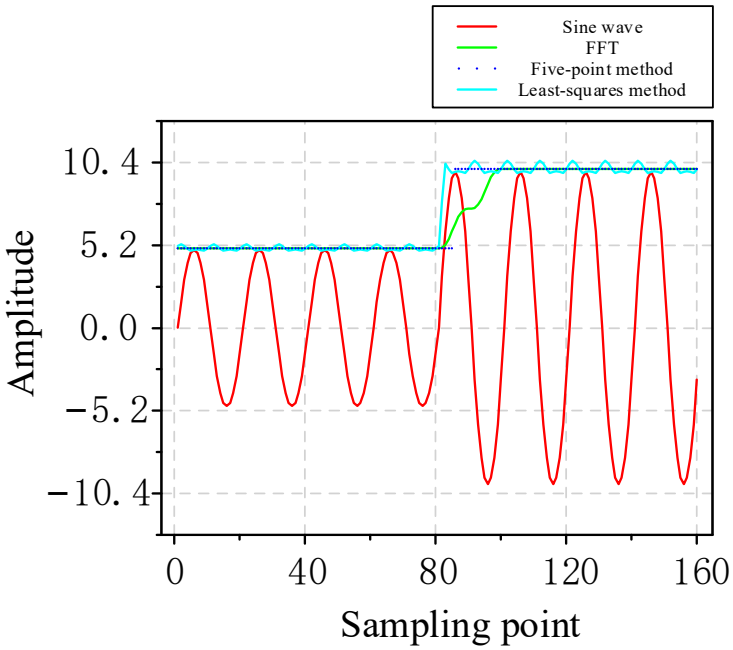


Figure 4. Sampled signal and estimated amplitude under dynamic variation with a third harmonic

B Experimental Validation

To assess the proposed method under physical measurement conditions, an indoor electric-field test platform was assembled, as shown in Figure 5. Parallel-plate electrodes generated a nominally uniform electric field, and a programmable high-voltage power supply controlled the excitation voltage between the plates.

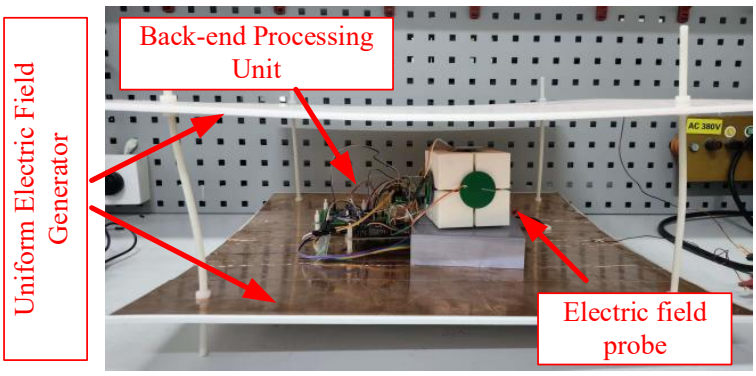


Figure 5. Power-frequency electric-field measurement platform

A custom electric-field measurement device was used to acquire the field between the plates. It consists of an electric-field probe and a back-end processing unit. The probe uses a parallel-plate capacitive structure to sense the field and produce a corresponding voltage. The back-end unit acquires and processes the signal and transmits the results wirelessly to a host computer for display and storage; its architecture is shown in Figure 6. The probe voltage is first amplified and conditioned by an AD620 instrumentation amplifier, then digitized by an AD7606 multichannel ADC. A microcontroller applies the five-point method to the digitized samples, and a wireless communication module sends the results to the host computer.

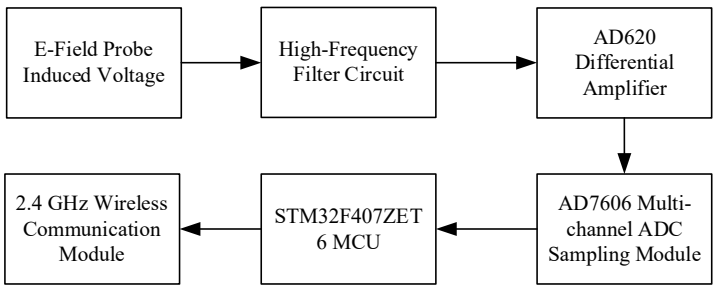


Figure 6. Block diagram of the back-end processing unit

The sampling interval was fixed at 1 ms. Discrete samples of the steady-state power-frequency electric field between the plates were collected and processed using the proposed five-point method and a conventional FFT; the results are shown in Figure 7. The five-point method uses the known power frequency as an input and estimates the parameters from five equally spaced samples, whose first-to-last time span is 4 ms. Both methods produced amplitude estimates near the theoretical value. The measured results fluctuated more than the ideal simulation results, mainly because of the finite bandwidth and offset voltage of the signal-conditioning amplifier and circuit noise.

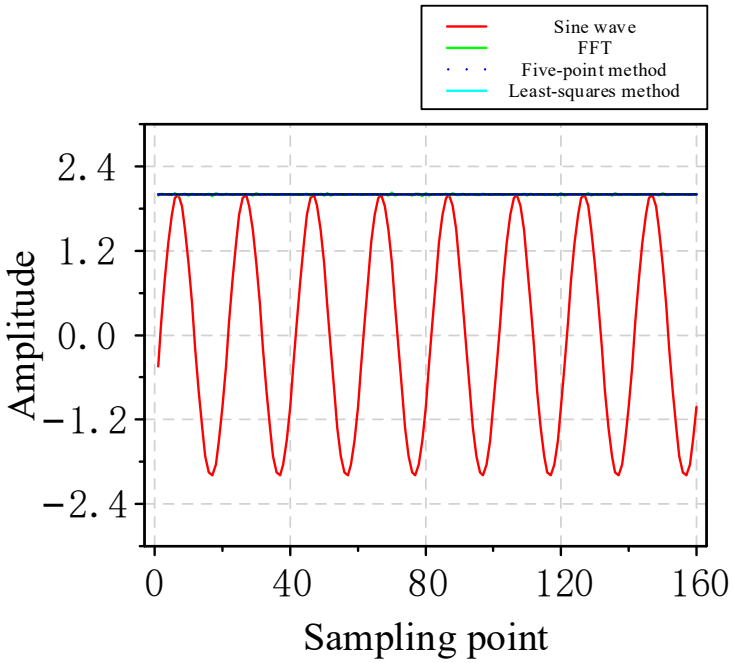


Figure 7. Sampled sinusoidal signal and estimated amplitude

To represent changes in electric-field amplitude as a UAV moves along a transmission line, the programmable high-voltage power supply was used to vary the sinusoidal voltage between the plates. The sampling interval remained 1 ms, and the five-point method and conventional FFT were used to estimate the signal parameters. The results are shown in Figure 8.

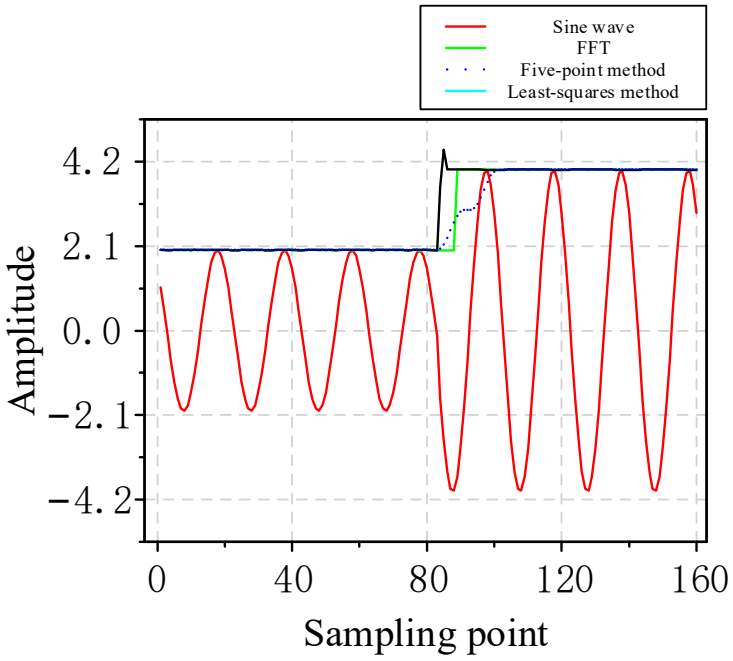


Figure 8. Sampled signal and estimated amplitude under dynamic variation

The measurements show that, under a time-varying electric field, the five-point method tracks amplitude changes using continuously updated sets of five samples. The first-to-last sample span is 4 ms, so the method can update its estimate without waiting for a complete 50 Hz cycle. The update rate of the conventional FFT depends on the analysis-window length and requires the corresponding samples to be collected. When the input amplitude changes, older and newer samples contribute to the same window, which can produce a transition or response delay.

Figures 7 and 8 show that the five-point method estimates power-frequency electric-field parameters in both steady-state and dynamic measurements, with trends consistent with the simulations. Its shorter sample span provides the basis for faster updates during amplitude changes. In practice, estimation accuracy is also affected by the sampling interval, signal noise, coefficient-matrix conditioning, and sensor calibration error.

VI Conclusions

This paper addressed short-window parameter estimation for transmission-line electromagnetic-field signals with a known fundamental frequency. A model comprising a DC component, a fundamental, and a third harmonic was linearized into sine and cosine coefficients. Five equally spaced samples were then used to form a 5×5 linear system, from which the DC component and the amplitudes and initial phases of the fundamental and third harmonic can be obtained. Because the solution matrix depends on the known frequency and sampling interval, it can be calculated in advance to reduce repeated computation during real-time processing.

MATLAB/Simulink simulations evaluated fundamental-only, third-harmonic, and time-varying-amplitude signals, and experiments using a power-frequency electric-field platform evaluated steady-state and dynamic measurements. With a 1 ms sampling interval, the first-to-last span of the five samples is 4 ms, allowing estimates to be updated without waiting for a full power-frequency cycle. Compared with the conventional FFT configuration used in this study, the five-point method uses a shorter data span and can provide faster updates when the field amplitude varies. Its dynamic performance depends on the sampling configuration and on how much the signal parameters change during the sample window.

The method assumes that the fundamental frequency is known and that the signal follows the stated model; it does not estimate frequency. A unique and reliable solution also requires a nonsingular, suitably conditioned coefficient matrix. An unsuitable sampling interval, unmodeled signal components, or substantial noise can increase estimation error. Future work will examine sampling-interval selection in relation to matrix conditioning and quantify estimation error, computation time, and noise sensitivity to establish the method's operating range in practical measurement systems.

Data availability

The datasets generated during and/or analysed during the current study are available from the corresponding author on reasonable request.

VII References

1. Suo, C. et al. Research on UAV three-phase transmission line tracking and localization method based on electric field sensor array. *Sensors* **21**, 8400 (2021). https://doi.org/10.3390/s21248400
2. Lee, G., Kim, J.-Y., Kim, G. & Kim, J. H. Surface-integrated electric field sensor for the detection of high-voltage power lines. *Sensors* **21**, 8327 (2021). https://doi.org/10.3390/s21248327
3. Wu, Y. et al. Overhead transmission line parameter reconstruction for UAV inspection based on tunneling magnetoresistive sensors and inverse models. *IEEE Trans. Power Deliv.* **34**, 819 – 827 (2019). https://doi.org/10.1109/TPWRD.2019.2891119
4. Satici, A. C., Peterson, A., Chiasson, J. & Adams, Z. Controlling UAVs by sensing the electric or the magnetic field around power lines. *IEEE Control Syst. Lett.* **7**, 3477 – 3482 (2023). https://doi.org/10.1109/LCSYS.2023.3334998
5. Salehi Rad, S. et al. Electromagnetic interference on unmanned aerial vehicles (UAVs): a case study of high power transmission line impacts. *IEEE Trans. Transp. Electrif.* **11**, 7501 – 7513 (2025). https://doi.org/10.1109/TTE.2025.3528188
6. Boukabou, I. & Kaabouch, N. Electric and magnetic fields analysis of the safety distance for UAV inspection around extra-high voltage transmission lines. *Drones* **8**, 47 (2024). https://doi.org/10.3390/drones8020047
7. Li, H., Stoica, P. & Li, J. Computationally efficient parameter estimation for harmonic sinusoidal signals. *Signal Process.* **80**, 1937 – 1944 (2000). https://doi.org/10.1016/S0165-1684(00)00103-1
8. Ramos, P. M., da Silva, M. F., Martins, R. C. & Cruz Serra, A. M. Simulation and experimental results of multiharmonic least-squares fitting algorithms applied to periodic signals. *IEEE Trans. Instrum. Meas.* **55**, 646 – 651 (2006). https://doi.org/10.1109/TIM.2006.864260

9. Ramos, P. M. & Cruz Serra, A. Least squares multiharmonic fitting: convergence improvements. *IEEE Trans. Instrum. Meas.* **56**, 1412 – 1418 (2007). https://doi.org/10.1109/TIM.2007.899873
10. Chen, K. F., Cao, X. & Li, Y. F. Sine wave fitting to short records initialized with the frequency retrieved from Hanning windowed FFT spectrum. *Measurement* **42**, 127 – 135 (2009). https://doi.org/10.1016/j.measurement.2008.04.007
11. Yu, K. K. C., Watson, N. R. & Arrillaga, J. An adaptive Kalman filter for dynamic harmonic state estimation and harmonic injection tracking. *IEEE Trans. Power Deliv.* **20**, 1577 – 1584 (2005). https://doi.org/10.1109/TPWRD.2004.838643
12. Xiao, X., Li, Z., Wang, Y. & Zhou, Y. A practical approach to estimate harmonic distortions in residential distribution system. *IEEE Trans. Power Deliv.* **36**, 1418 – 1427 (2021). https://doi.org/10.1109/TPWRD.2020.3008700
13. Wang, Y. et al. Harmonic state estimation for distribution networks based on multi-measurement data. *IEEE Trans. Power Deliv.* **38**, 2311 – 2325 (2023). https://doi.org/10.1109/TPWRD.2023.3239479
14. Belega, D., Petri, D. & Dallet, D. Amplitude and phase estimation of real-valued sine wave via frequency-domain linear least-squares algorithms. *IEEE Trans. Instrum. Meas.* **67**, 1065 – 1077 (2018). https://doi.org/10.1109/TIM.2017.2785098
15. Belega, D. & Petri, D. Cramér-Rao lower bound for unbiased estimators of sampled noisy sine-wave parameters. *IEEE Trans. Instrum. Meas.* **70**, 1 – 9 (2021). https://doi.org/10.1109/TIM.2021.3122791
16. Belega, D. & Petri, D. Fast procedures for accurate parameter estimation of sine-waves affected by noise and harmonic distortion. *Digit. Signal Process.* **114**, 103035 (2021). https://doi.org/10.1016/j.dsp.2021.103035
17. Lin, J., Chan, S. C. & Wu, H.-C. A robust PAST-based ESPRIT algorithm with variable forgetting factor and regularization for frequencies/harmonics estimation in impulsive noise. *IEEE Trans. Instrum. Meas.* **71**, 6502213 (2022). https://doi.org/10.1109/TIM.2022.3173613
18. Song, J., Mingotti, A., Zhang, J., Peretto, L. & Wen, H. Accurate damping factor and frequency estimation for damped real-valued sinusoidal signals. *IEEE Trans. Instrum. Meas.* **71**, 1 – 4 (2022). https://doi.org/10.1109/TIM.2022.3220300
19. Corrêa Alegria, F. Uncertainty of the initial phase estimation of a sinewave in the presence of phase noise, additive noise or jitter. *J. Franklin Inst.* **361**, 107116 (2024). https://doi.org/10.1016/j.jfranklin.2024.107116
20. Macii, D. et al. Single-cycle P class phasor estimation based on harmonics whitening and off-nominal frequency offset adjustment. *Electr. Power Syst. Res.* **229**, 110119 (2024). https://doi.org/10.1016/j.epsr.2024.110119
21. Jia, W., Wang, C. & Xiang, J. A novel approach to estimating harmonic/interharmonic parameters. *Measurement* **240**, 115586 (2025). https://doi.org/10.1016/j.measurement.2024.115586
22. Barzegar, M. & Alegria, F. Experimental validation of the precision of sinusoidal amplitude estimation using a least squares procedure in the presence of additive noise. *Sci. Rep.* **15**, 12789 (2025). https://doi.org/10.1038/s41598-025-95861-7

Acknowledgements

This work was supported by the Science and Technology Project of State Grid Fujian Electric Power Company. (Grant No. 52130425000T), titled "Research and Application of UAV Autonomous Inspection Technology Based on the Fusion of Electromagnetic Field Detection and Target Recognition." The authors also acknowledge the technical support and contributions provided by the project team members.

Author contributions

W.Z. conceived and designed the study, developed the methodology, secured funding, and wrote the original manuscript. W.W., X.W., and R.W. conducted the experiments, collected and analyzed the data, and prepared the figures. All authors reviewed and approved the final manuscript.

Funding

This work was supported by the Science and Technology Project of State Grid Fujian Electric Power Company. (No. 52130425000T): Research and Application of UAV Autonomous Inspection Technology Based on the Fusion of Electromagnetic Field Detection and Target Recognition.

Competing interests

The author(s) declare no competing interests.